Biochimica et Biophysica Acta 1848 (2015) 1955–1962

Contents lists available at ScienceDirect

Biochimica et Biophysica Acta

journal homepage: www.elsevier.com/locate/bbamem

Binding structure and kinetics of surfactin monolayer formed at the air/water interface to counterions: A molecular dynamics simulation study

Hongze Gang [a], Jinfeng Liu [a], Bozhong Mu [a,b,*]

[a] State Key Laboratory of Bioreactor Engineering and Applied Chemistry Institute, East China University of Science and Technology, 130 Meilong Road, Shanghai 200237, PR China
[b] Shanghai Collaborative Innovation Center for Biomanufacturing Technology, 130 Meilong Road, Shanghai 200237, PR China

ARTICLE INFO

Article history:
Received 21 March 2015
Received in revised form 9 May 2015
Accepted 19 May 2015
Available online 27 May 2015

Keywords:
Surfactin monolayer
Counterion
Binding affinity
Salt bridge
Break rate

ABSTRACT

The binding structure and kinetics of ionized surfactin monolayer formed at the air/water interface to five counterions, Li^+, Na^+, K^+, Ca^{2+}, and Ba^{2+} (molar ratios of surfactin to monovalent and divalent counterions are 1:2 and 1:1 respectively), have been studied using molecular dynamics simulation. The results show that surfactin exhibits higher binding affinity to divalent counterions, Ca^{2+}, and Ba^{2+}, and smaller monovalent counterion, Li^+, than Na^+ and K^+. Both carboxyl groups in surfactin are accessible for counterions, but the carboxyl group in Glu1 is easier to access by counterions than Asp5. Salt bridges are widely built between carboxyl groups by counterions, and the probability of the formation of intermolecular salt bridge is markedly larger than that of intramolecular salt bridge. Divalent counterions perform well in forming salt bridges between carboxyl groups. The salt bridges mediated by Ca^{2+} are so rigid that the lifetimes are about 0.13 ns, and the break rates of these salt bridges are 1–2 orders of magnitude smaller than those mediated by K^+ which is about 5 ps in duration. The positions of the hydration layer of carboxyl groups are independent of counterions, but the bound counterions induce the dehydration of carboxyl groups and disturb the hydrogen bonds built between carboxyl group and hydration water.

1. Introduction

Surfactin, a family of cyclic lipopeptides produced by several strains of *Bacillus subtilis* [1–3], attracts more attention for their potential applications in food and cosmetic [4], remediation of petroleum contaminated soil [5], neurodegenerative disorder disease therapy [6], and enhanced oil recovery [7] owing to their predominant surface property [8,9] and special biological activities, such as antimicrobial [3], antiviral [10], antifungal [11], and hemolytic properties [12]. The two acidic amino acid residues in the peptide moiety, Glu1 and Asp5, were considered as the hydrophilic group of surfactin [13] and the physical state of the two carboxyl groups in these residues dramatically affected surfactin properties, such as spatial arrangement of surfactin at interface and in solution which were relative to lowering surface tension and the change of critical micelle concentration (CMC) [14–19], interaction affinity with membrane regarding to hemolysis [20], and chelating capacity of cations involved in inhibiting enzyme activity [21], etc. Counterion is one of the extrinsic environmental factors that are important in affecting the physical state of $—COO^-$ groups in Glu1 and Asp5, therefore the interaction between ionized surfactin and counterions is crucial in designing suitable, stable, and effective applications of surfactin.

According to the pK values of surfactin in solution or at interface [14,22], more than 90% of surfactin has a dianionic form when pH >5. The effective charge of the $—COO^-$ groups in Glu1 and Asp5 depends on the type and concentration of counterion. The surface activity of surfactin was enhanced by the addition of counterions in reducing CMC values and lowering the surface tensions at CMC [17,20]. The morphology of surfactin aggregates was induced by divalent counterions from spherical micelle to larger aggregates in rod-like or lamellar shape, which were demonstrated by the binding of carboxyl groups to divalent counterions and the subsequent screening of electrostatic repulsion between surfactin molecules in micelle [16]. Surfactin exhibited much higher binding affinity to divalent counterions than monovalent counterions [17]. The $—COO^-$ groups of surfactin monolayer at air/aqueous interface were more completely neutralized by adding divalent counterions in the subphase estimated by the shape of the isotherm curves and the characteristic values from the curves [14]. Small angle neutron scattering measurement showed that the bulk phase structure of surfactin was changed by counterions in an order of $Li^+/K^+ < Ca^{2+} < Ba^{2+}$ due to the stable and more hydrophobic complex between surfactin and divalent counterions [16]. Biological properties of surfactin are affected by counterions as well. The formation of surfactin–counterion complex was considered as the factor of the inhibition of alkaline phosphatase by surfactin because the

* Corresponding author at: State Key Laboratory of Bioreactor Engineering and Applied Chemistry Institute, East China University of Science and Technology, 130 Meilong Road, Shanghai 200237, PR China.
E-mail address: bzmu@ecust.edu.cn (B. Mu).

http://dx.doi.org/10.1016/j.bbamem.2015.05.016
0005-2736/

enzyme needed Zn^{2+} and Mg^{2+} to keep its activity [21]. The increase of surfactin hemolysis was induced by the presence of very low concentrations of divalent counterions or higher concentrations of monovalent counterions, which meant that surfactin was favored to interact with erythrocyte membrane after binding to counterions [20]. As summarized above the binding of ionized surfactin to counterions was studied by measuring the change in surfactin CMC, surface tension at CMC, micellar morphology, and the apparent biological activities, but the details of the binding structure between surfactin and counterions, and the insights of binding affinity of surfactin to different counterions are still limited and need to be further investigated.

In the present work, molecular dynamics simulation had been used to get the atomistic details of the binding of surfactin monolayer formed at the air/water interface to three monovalent counterions (molar ratio of surfactin:counterions = 1:2), Li^+, Na^+, K^+, and two divalent counterions (molar ratio of surfactin:counterions = 1:1), Ca^{2+} and Ba^{2+}. The binding structure between ionized surfactin and counterions was studied by both radial and spatial distribution functions of counterions and water molecules around carboxyl groups in the two acidic amino acid residues of surfactin. The binding affinity to monovalent and divalent counterions was analyzed by comparing the bound fraction of counterions, screening the structure of salt bridge between carboxyl groups mediated by counterions, and also the kinetic revolutions of the binding of surfactin to counterions and the salt bridge formed between carboxyl groups.

2. Computational details

Surfactin used in the present simulation is *iso*-C15 surfactin (15 denotes the carbon number in the β-hydroxyl fatty acid moiety) in dianionic form, and its chemical structure is given in Fig. 1a. The backbone of the peptide ring adopts a "horse-saddle" conformation characterized by Bonmatin et al. [13] by means of NMR combined with molecular modeling, which can be seen in Fig. 1b. Here the peptide ring moiety is considered as surfactin headgroup, and the remainder aliphatic chain from the γ carbon atom is taken as surfactin tail. A series of simulations was performed for ionized surfactin monolayer formed at the air/water interface with different counterions. Ionized surfactin number was fixed with 32, and the interfacial area of surfactin molecule at the air/water interface was set as 1.5 nm^2/molecule, corresponding to the limiting molecular area (A_0) of surfactin obtained in experimental studies [16,24,25] and also the most probable interfacial area of surfactin calculated by molecular dynamics simulations [26,27].

The setup steps of all the simulations were the same as follows. Firstly, a box ($L_x \times L_y \times L_z$: 4.9 nm × 4.9 nm × 5 nm) was filled with SPC (Single Point Charge) water molecules [28] and equilibrated at 298 K for 300 ps, and then the water box was centered in a cube which had the same L_x and L_y dimensions and a size of 15 nm in z direction. Secondly, two 4 × 4 surfactin layers were separately placed on the two air/water interfaces with their ionized amino acid residues, Glu1 and Asp5, and most of their peptide ring backbone solvated. After that, certain number of the inorganic counterions (64 monovalent counterions or 32 divalent counterions) was introduced into the system by randomly replacing the water molecules by counterions to neutralize the system, and energy minimization was performed using the steepest descent. Thirdly, a period of 20 ns MD simulation was applied to the systems by a time step of 2 fs, and the equilibration of the simulation was checked by monitoring the potential energy as well as the root-mean-square deviation of the peptide ring backbone.

The Gromacs 3.3.1 package [29,30] and the OPLS-aa force field [31] were used to run all the MD simulations in the NVT ensemble. Berendsen thermostat [32] was applied to maintain the system temperature at 298 K, and the coupling time constant was 0.1 ps. The cutoff radius of both van der Waals interactions and the real part of electrostatic interactions was 1.0 nm. Electrostatic forces were calculated using particle mesh Ewald method [33] with precision 10^{-4}. All bond lengths were constrained using LINCS algorithm [34] with an order of 4, and the periodic condition was applied in all the three directions. MD trajectories were collected every 1.0 ps and the last 10 ns run was used for analysis. Additional 500 ps simulations were performed for ultrafast properties such as hydrogen bond and salt bridge dynamics, and the time interval was 10 fs for data collection.

3. Results

3.1. Binding structure between —COO^- group and counterion

The binding structure between ionized surfactin and counterions was firstly analyzed by the radial distribution functions (RDFs) of counterions around the oxygen atoms in —COO^- groups, $g(r)_{-COO^-\text{-counterions}}$, which are shown in Fig. 2a. Definite peaks are observed from all the RDF curves which mean that adsorption shells are formed by bound counterions around —COO^- groups. The positions of adsorption shells are proportional to the Lennard–Jones parameters of each counterion, σ, which describes the interaction size of ions in the present simulation (inset plot in Fig. 2a). Comparing with the positions of the hydration layers of carboxyl groups, which are about 0.27 nm from $g(r)_{-COO^-\text{-Ow}}$ (Fig. 2b), the adsorption shells of Li^+, Na^+, and Ca^{2+} are mostly within the hydration layer, while the adsorption shells of K^+ and Ba^{2+} are simultaneously presented with the hydration layer. More compact adsorption shells are formed by counterions that have higher valence and bigger Lennard–Jones parameters ε (thickness of adsorption shells is listed in Table 1), Ca^{2+} and Ba^{2+} for example, and result in lower number of counterions resided in the adsorption shells (Table 1). However, the thinner adsorption shells of divalent counterions are higher charged comparing with that of monovalent counterions when taking

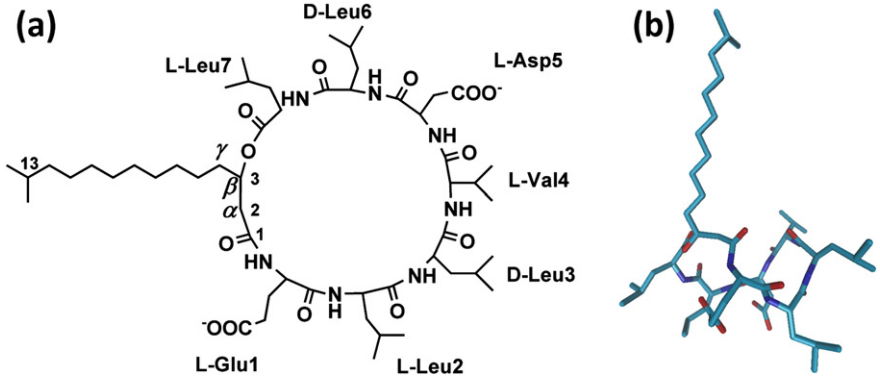

Fig. 1. (a) Primary structure of ionized *iso*-C15 surfactin; (b) "horse saddle" conformation of surfactin, oxygen: red, nitrogen: blue, carbon: cyan, all the hydrogen atoms are not shown for clear display. Conformational images in this paper are all produced by VMD software [23].

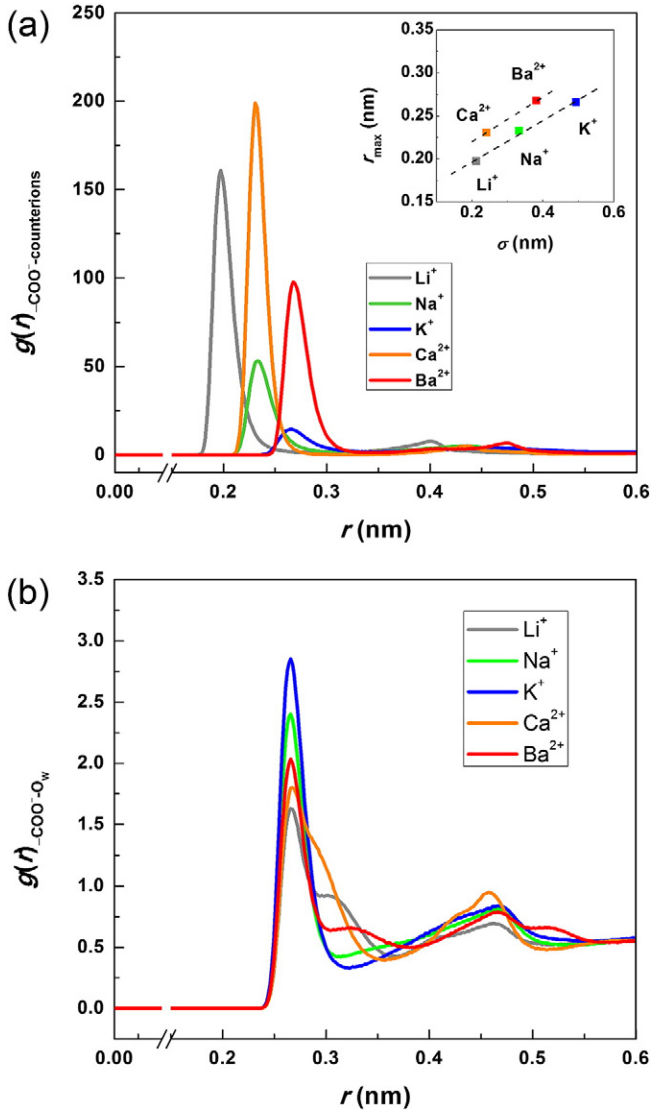

Fig. 2. (a) Radial distribution functions of counterions around oxygen atoms in —COO^- groups. Inset plot is the comparison between Lennard–Jones parameters of counterions used in the present simulation and the first maximum radius in RDFs, r_{max}. (b) Radial distribution functions of water oxygen atoms around the oxygen atoms in —COO^- groups.

valence into account. Higher van der Waals interaction and electrostatic attractions between oxygen atom in carboxyl groups and divalent counterion are responsible for the compact adsorption shells.

The spatial distributions of counterions and water molecules around ionized carboxyl group of surfactin are displayed in Fig. 3. It can be easily identified that smaller monovalent counterion, Li^+, exhibits a wider spatial distribution than those of Na^+ and K^+ which graphically illustrates the peak intensities of RDFs in Fig. 2a. Both divalent counterions, Ca^{2+} and Ba^{2+}, show more concentrate spatial distribution comparing with monovalent counterions, which means stronger interaction and thus more stable binding structure between carboxyl group and divalent counterion. Hydration water has more spatial and orientational choice in interacting with carboxyl groups where there are fewer counterions that resided in the adsorption shells, as shown in Fig. 3b, c, and the left half of Fig. 3e. As a result, the number of hydration water is higher which can be found from RDFs in Fig. 2b, and more hydrogen bonds are formed between carboxyl group and hydration water with higher energy as summarized in Table 1. In contrast, the structures of the hydration layers are disturbed by Li^+ and Ca^{2+} resulting in fewer and less stable hydrogen bonds, because the approaching of water molecules to oxygen atoms in carboxyl groups is affected by the repulsion between hydrogen atom in water and bound counterion.

3.2. Binding affinity of surfactin to counterions

According to the first minimum values in $g(r)_{-COO^-\text{-counterions}}$, r_{min}, the bound state of two —COO^- groups of surfactin was screened to get the binding fractions of ionized surfactin in the presence of different counterions. Fig. 4a gives the fractions of free (both —COO^- groups in Glu1 and Asp5 are free of counterions), semi-bound (only one of the two —COO^- groups in surfactin is bound with counterion), and fully-bound (both —COO^- groups in Glu1 and Asp5 are bound with counterions) surfactin, and it seems that surfactin prefers to bind to counterions with smaller radii and higher valence. When it comes to the semi-bound surfactin, more than half of them bind to counterions with the —COO^- group in Glu1 (Fig. 4b) illustrating higher binding affinity to counterions of Glu1 compared with Asp5. For the fully-bound surfactin, the two —COO^- groups have priority to bind to different counterions separately, only a few surfactin bind to one counterion to form an intramolecular salt bridge (Fig. 4b). It should be noticed that the number of intramolecular salt bridge is considerable in the presence of Ba^{2+}, and this result is mostly relative to the higher valence and the largest radius of Ba^{2+}, which benefits the neutralization of the two —COO^- groups and prevents the higher steric energy of surfactin binding to one Ba^{2+} ion.

The effective charge of surfactin (originally $2e$) in the monolayer is obtained using the bound fractions of counterions given in Fig. 4c. The negative charge of ionized surfactin is mostly neutralized by Li^+ ($0.08e$) and Ba^{2+} ($0.11e$), and completely neutralized by Ca^{2+} ($0e$), while partly neutralized in the case of Na^+ ($0.76e$) and K^+ ($1.20e$). Independent of valence and radii, bound counterions exhibit priority in forming intermolecular salt bridge than intramolecular salt bridge since one —COO^- can easily access another —COO^- of the adjacent surfactin by rotating or orienting the surfactin headgroups at the air/water interface to share one counterion (Fig. 4c). Diffusion mobility of counterions also provides indications of binding affinity of ionized surfactin to counterions. As can be seen in Fig. A.1, most of Li^+, Ca^{2+}, and Ba^{2+} that have very small vertical diffusion coefficients, D_{zz}, which are 1–2 orders slower than the diffusion coefficient of bulk water at the same temperature [35], are the bound counterions. The higher binding affinity of ionized surfactin to divalent counterions and smaller monovalent counterion is clearly displayed in Fig. 5 that Ca^{2+},

Table 1
Thicknesses of adsorption shells of bound counterions around oxygen atoms in —COO^- groups, the averaged numbers of counterions reside in adsorption shells, averaged number and energy of hydrogen bonds (HBs) formed between —COO^- groups of surfactin and water molecules in hydration layer.[a]

System	$(Li^+)_2SF^{2-}$	$(Na^+)_2SF^{2-}$	$(K^+)_2SF^{2-}$	$Ca^{2+}SF^{2-}$	$Ba^{2+}SF^{2-}$
Shell thickness (nm)	0.123	0.117	0.112	0.107	0.103
Counterions in shells[b]	1.12	0.65	0.32	0.78	0.70
Number of HB	0.80	1.11	1.36	0.84	1.02
HB energy (kJ/mol)	16.9	18.3	18.5	17.0	17.9

[a] The first minimum radius in RDF curves in Fig. 2b, r_{min}, is the distance threshold between hydrogen donor and hydrogen acceptor, and an angle of 30° is set as angular threshold to define the hydrogen bonds formed between —COO^- groups of surfactin and water molecules in the hydration layer.
[b] Integration of RDF profiles in Fig. 2a up to the first minimum radius, r_{min}.

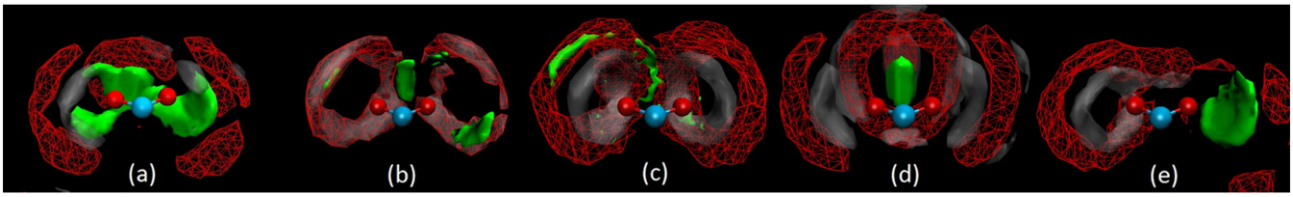

Fig. 3. Spatial distribution of counterions (green solid), water oxygen atoms (red frame), and water hydrogen atoms (white transparent) around one of the carboxyl groups (carbon atom: cyan; oxygen atom: red) in surfactin ions in systems (a) $(Li^+)_2SF^{2-}$; (b) $(Na^+)_2SF^{2-}$; (c) $(K^+)_2SF^{2-}$; (d) $Ca^{2+}SF^{2-}$; and (e) $Ba^{2+}SF^{2-}$. Isosurface values are 80 for water oxygen atoms, 80 for water hydrogen atoms, and 1500 for counterions.

Ba^{2+}, and Li^+ are mostly restrained within surfactin headgroup regions, and some of Na^+ and K^+ ions away from surfactin are the free counterions corresponding to those with bigger values of D in Fig. A.1b and c.

3.3. Kinetics of binding of surfactin to counterions and salt bridge mediated by counterions

The kinetic evolution of binding of surfactin to counterions and salt bridges between carboxyl groups mediated by counterions is analyzed by two time correlation functions (TCFs) which are employed to study the kinetics of hydrogen bonds [35–38],

$$S(t) = \frac{\langle h(0)\cdot H(t)\rangle}{\langle h\rangle} \tag{1}$$

and

$$C(t) = \frac{\langle h(0)\cdot h(t)\rangle}{\langle h\rangle} \tag{2}$$

where $S(t)$ and $C(t)$ are the continuous and intermittent time correlation functions, respectively. $H(t)$ is a binary function which is equal to 1 if a set of binding sites continuously bound up to time t, and the binary function $h(t)$ is 1 when the monitored sites keep binding at time t and the binding is allowed to be broken within the time interval 0–t. $<>$ means the average over all the time points and all the binding sites. The thresholds are whether the counterion is within the adsorption shell of one carboxyl group for binding, and whether the counterion resides in the adsorption shells of two —COO^- groups for salt bridge. Therefore, we can get the lifetime and structural stability of binding structure and salt bridge from $S(t)$ and $C(t)$ respectively.

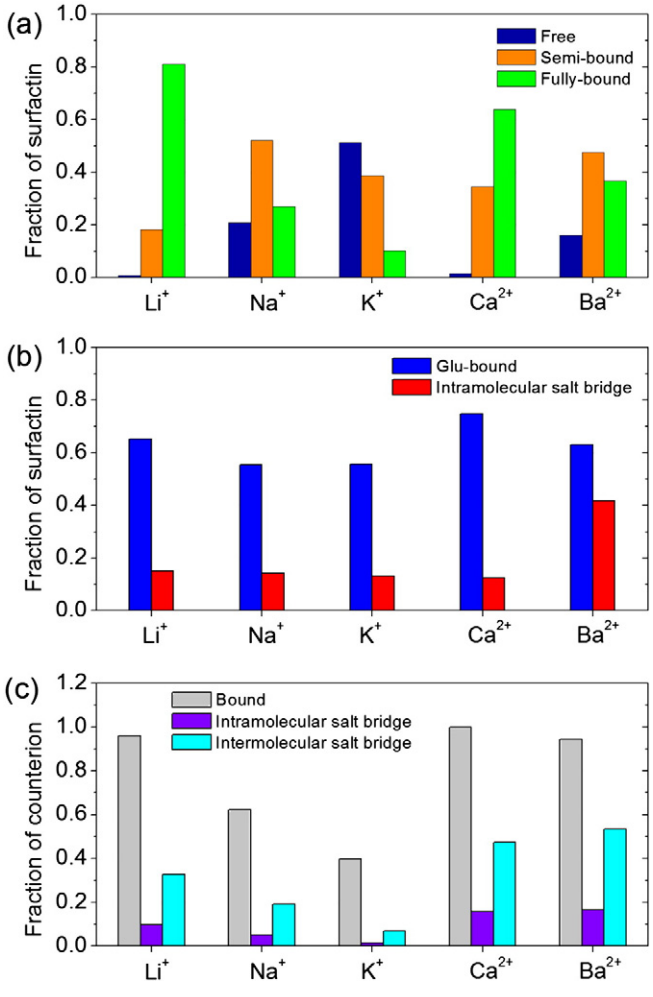

Fig. 4. (a) Fractions of ionized surfactin that both —COO^- groups are free of counterions, one of the —COO^- groups is bound with counterion, and two —COO^- groups are fully bound with counterions; (b) fractions of ionized surfactin that only —COO^- group in Glu1 is bound out of semi-bound surfactin, and fractions of ionized surfactin that two —COO^- groups bind to one counterion to form intramolecular salt bridge out of fully-bound surfactin. (c) Fraction of bound counterion and counterions participating in formation of intramolecular salt bridge or intermolecular salt bridge.

TCFs of binding of surfactin to counterions can be seen in Fig. 6 (TCFs of intramolecular and intermolecular salt bridges are given in Figs. A.2 and A.3). Nearly all the TCFs show the relaxation in an order of $K^+ > Na^+ > Ba^{2+} \sim Li^+ > Ca^{2+}$, indicating that the strength of the binding between counterion and surfactin decreases in the order of $Ca^{2+} > Li^+ \sim Ba^{2+} > Na^+ > K^+$, which is in the same tendency of the binding affinity of surfactin to counterions previously obtained in Section 3.2. Much slower relaxations of $C(t)$ comparing with those of $S(t)$ demonstrate that the counterions stay within or nearby the headgroup region even after the break-up of binding or salt bridge, which benefits the reform of binding or salt bridge sometime. A sum of three exponential functions, $\sum_{i=1}^{3} A_i \exp(-t/\tau_i)$, is used to fit the curves of $S(t)$ and $C(t)$, and the lifetimes of binding and salt bridge are obtained by $\sum_{i=1}^{3} A_{Si}\tau_{Si}$ (Table 2). The most rigid binding and salt bridge are formed between surfactin and Ca^{2+} and the lifetimes are about 0.13 ns, which are about twice of those in $(Li^+)_2SF^{2-}$ and $Ba^{2+}SF^{2-}$ systems, and nearly ten times longer than that mediated by K^+. Fluctuations in TCFs in Fig. A.2 are caused by the smaller number of intramolecular salt bridges and thus the rough statistic results.

For an existing binding between one carboxyl group and one counterion, the relaxation of its continuous time correlation function depends on the break rate, $k_S(t)$, which can be written as

$$-\frac{dS(t)}{dt} = k_S(t). \tag{3}$$

Combined with $S(t) = \sum_{i=1}^{3} A_{Si}\exp(-t/\tau_{Si})$, $k_S(t)$ can be obtained by

$$k_S(t) = \sum_{i=1}^{3} \frac{A_{Si}}{\tau_{Si}} \exp(-t/\tau_{Si}). \tag{4}$$

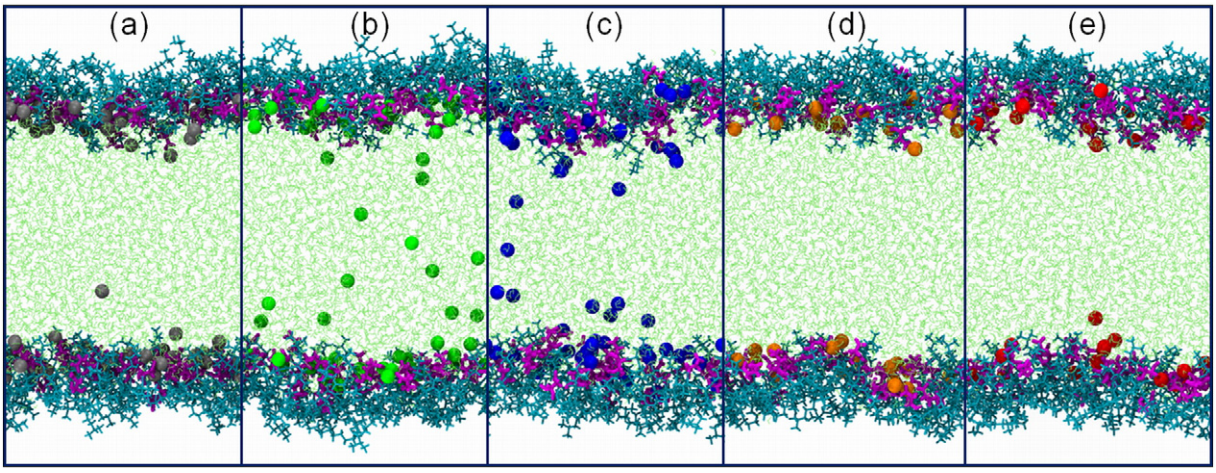

Fig. 5. Snapshots of counterion location (a) Li^+, (b) Na^+, (c) K^+, (d) Ca^{2+}, and (e) Ba^{2+}.

Similarly, the relaxation of intermittent time correlation function relates to $k_C(t)$ which can be derived as $k_C(t) = \sum_{i=1}^{3} \frac{A_{Ci}}{\tau_{Ci}} \exp(-t/\tau_{Ci})$. As shown in Fig. 6 and Figs. A.2 and A.3, all the break rates slightly decrease at first and then markedly drop as a function of time, and the latter drop of break rates can be mainly attributed to the rapid reduction of binding structures or salt bridges. From the beginning to 50 ps there are abundant binding structures and salt bridge, it can be quantitatively concluded that the break rates of the most rigid binding structure and salt bridge between surfactin and Ca^{2+} are in an order of 10^{-3} ps^{-1}, while the break rates of those with the lowest stability in the presence of K^+ are 1–2 orders higher than those mediated by Ca^{2+}. All the $k_C(t)$ are much smaller than the corresponding $k_S(t)$ further proving that counterions reside nearby the carboxyl groups after the break-up of binding structure or salt bridge and the rebuilds of binding structures and salt bridges are facilitated. The typical snapshots in Fig. 7 show the stable binding of surfactin to Li^+ and the rigid intermolecular salt bridge mediated by Ca^{2+} by spatial distribution of counterions around the ionized carboxyl groups.

4. Discussion

In the present study, it is illustrated that the positions of the hydration layers of —COO^- groups are independent of counterions, but the counterions induce the dehydration of hydration layer of carboxyl group. Fewer hydrogen bonds with smaller energy were formed between carboxyl group and hydration water in the presence of highly bound counterions as Ca^{2+}, Ba^{2+}, and Li^+. Results of neutron reflection [16] showed that there were less water molecules in the headgroup region of surfactin monolayer in the presence of Ca^{2+} and Ba^{2+} which

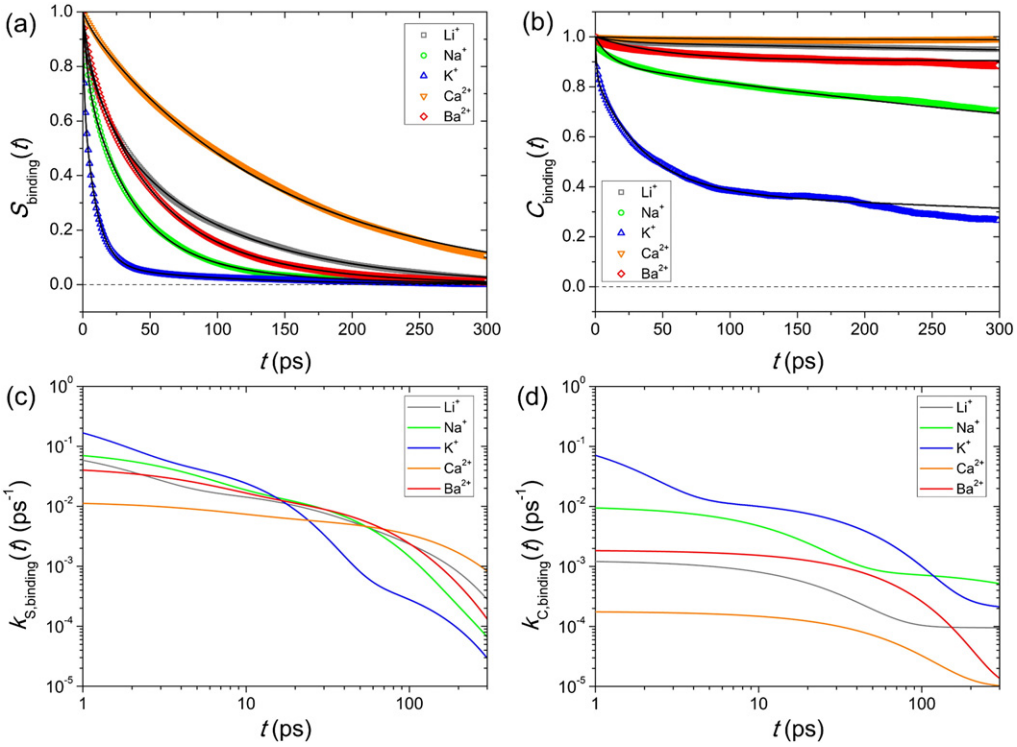

Fig. 6. (a) Continuous time correlation functions, (b) intermittent time correlation functions, (c) break rates, $k_S(t)$, and (d) break rates, $k_C(t)$ for the binding of ionized carboxyl groups of surfactin to counterions. The solid lines in (a) and (b) are the fitting of time correlation functions by three exponential functions.

Table 2
Lifetime of binding and salt bridge formed between counterions and ionized carboxyl groups of surfactin.

System	Lifetime (ps)		
	Binding	Intramolecular salt bridge	Intermolecular salt bridge
$(Li^+)_2SF^{2-}$	64.5	81.6	85.7
$(Na^+)_2SF^{2-}$	35.4	14.7	31.9
$(K^+)_2SF^{2-}$	13.0	4.7	5.0
$Ca^{2+}SF^{2-}$	138.7	134.2	131.2
$Ba^{2+}SF^{2-}$	52.0	55.4	42.9

were highly bound to surfactin comparing with monovalent counterions. The disturbance of hydration layer by counterions that penetrate into hydration layer was observed in traditional surfactant monolayer formed at the air/water interface [39]. Moreover, partly dehydrated state of surfactants was calculated to charge of the varying abilities of several surfactants to discriminate different cations [40].

The bound fraction of counterions increases with the decrease of ion radius for both monovalent and divalent counterions in the present simulation, and this can be demonstrated by the smaller lateral electrostatic repulsion between the bound counterions which are restricted in the headgroup region of surfactin monolayer. In the investigation of the self-assembly of surfactin in aqueous solution affected by divalent counterions, it was found that smaller counterions with higher eletronegativity have higher degree of association with surfactin [19]. Higher binding degree of small monovalent ion Li^+ than K^+ had also been found by studying surfactin micellization in the presence of counterions [16]. Although the binding of surfactin to monovalent counterions was lower than divalent counterions, the binding was proposed to reach an equilibrium state [14] and the free fraction of the surfactin at air/water interface was around 0.3–0.4 in the presence of K^+ or Na^+. The fractions of free surfactin and semi-free surfactin we get here are 0.208 and 0.522 in the presence of Na^+, 0.512 and 0.386 in the case of K^+, which are higher than the experimental results mainly due to the much higher ratios of surfactin to counterions in the present simulation whereas the salt was in excess in the previous experimental study.

The special structure of surfactin headgroups is proposed to be a factor that markedly affects the binding of surfactin to counterions since the spatial cavities are provided by the backbones of headgroups which exposed two anchors, carboxyl groups in Glu1 and Asp5, to the aqueous solution. Take Li^+ ion for example, smaller monovalent counterions need smaller cavities to penetrate into the headgroup region and be bound to carboxyl groups, resulting in higher binding fractions. In the investigation of binding selectivity of iturin A_2, an analogue of lipopeptide owned a peptide ring in the molecule as well, to alkali metal ions, the binding order $Na^+ > K^+ > Rb^+$ was mainly caused by the size limitation in interaction cavity [41]. It was assumed that only one of the two —COO^- groups of surfactin peptide moiety was accessible due to the smaller binding fraction of monovalent counterions [14]. The presenting results firstly demonstrate that both carboxyl groups are accessible for counterions, but the carboxyl group in Glu1 has better accessibility to either monovalent or divalent counterions. It is probably resulted from the longer chain of Glu1 compared with Asp5 and thus the more flexible orientation of Glu1 to bind to counterions. It is also possible that the binding of —COO^- in Glu1 to one counterion inhibits or affects the binding of —COO^- in Asp5 to a second counterion.

Higher participation of divalent counterions, Ca^{2+} and Ba^{2+}, in binding and salt bridge can be demonstrated by their higher valence that can largely neutralize the negative charge of surfactin and their larger radius to form salt bridges between carboxyl groups, and the bidentate sites of the peptide moiety of surfactin as well. Higher binding fractions of divalent counterions than monovalent counterions were obtained in many experimental studies. The neutralization of the surfactin monolayer adsorbed at the air/water interface seemed complete by Ca^{2+} but incomplete in the case of monovalent counterions, K^+ or Na^+ [14]. The hydrophobicity of surfactin headgroup at air/water interface was enhanced by divalent counterions leading to the larger separation between two acidic amino acid residues and water estimated by the fitting of neutron reflectivity profiles [16]. The binding selectivity of divalent counterions was observed in surfactin micellar structure as well. The study of Li et al. [17] showed that at low concentration of divalent counterions surfactin formed larger aggregations which might be caused by the assembly of surfactin micelles indicating a more neutralization of micelle by divalent counterions. Small angle neutron scattering of surfactin micelle [16] showed that surfactin micellar size and morphology were independent with monovalent counterions even at extra high ratio of counterion to surfactin, but more sensitive to divalent counterions. In a biological aspect, the binding affinity of surfactin to Ca^{2+} is related to its interaction with the membrane [42], and the deep insertion of surfactin into phospholipid bilayer is facilitated since the electrostatic repulsion between lipid headgroup and surfactin peptide moiety is reduced [43].

It was presumed that the formation of surfactin–cation 1:1 complex, in which a salt bridge between two carboxyl groups was mediated by divalent counterion, accounted for the stronger strength of the binding between ionized surfactin and divalent counterions [14]. Slower decay of the binding structure between surfactin and Ca^{2+} was observed comparing with those between surfactin and Ba^{2+}, which indicated

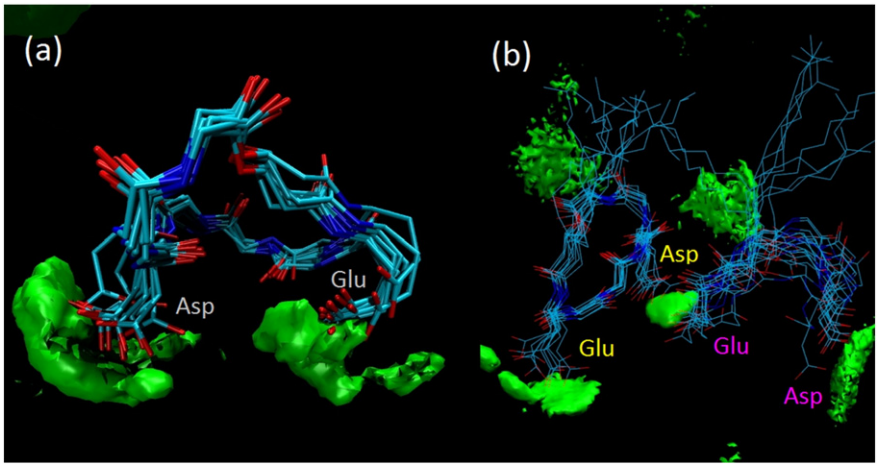

Fig. 7. Spatial distribution of counterions (green solid) around ionized surfactin in (a) $(Li^+)_2SF^{2-}$, where only the backbone of headgroup and the two acidic amino acid residues are shown, and (b) $Ca^{2+}SF^{2-}$, where the hydrophobic amino acids are not displayed. C, N, and O atoms in ionized surfactin are shown in cyan, blue, and red, for clear display all the hydrogen atoms are omitted.

that Ca^{2+} had a stronger interaction with surfactin than Ba^{2+}. However, Shen et al. [16] reported that Ba^{2+} has a stronger interaction than Ca^{2+} from small angle neutron scattering measurements. The difference is probably caused by the different structures of surfactin aggregate at air–water interface and in bulk solution. Surfactin formed aggregates in bulk solution, and the molecular area of surfactin in micelle was about 3.9 nm^2 according to the diameter and the aggregation number of surfactin micelle [44], which was remarkably larger than the interfacial area at the air–water interface used in the present MD simulations, 1.5 nm^2/molecule. Therefore, the larger distance between $—COO^-$ groups in surfactin micelle facilitated the binding of surfactin to divalent counterions that have bigger radius, such as Ba^{2+}. The formation of salt bridge was widely detected in the present simulation, even in the presence of monovalent counterions which were not considered or suggested to form salt bridge with surfactin in the previous research. Salt bridges mediated by Ca^{2+} and Ba^{2+} were numerically more than those mediated by monovalent counterions, because divalent counterions with higher valence and the larger radius interact with the two $—COO^-$ groups intensively and without higher steric repulsion. Salt bridge between surfactant headgroups near the air/water interface was built in monolayers of sodium dodecyl carboxylate and sodium dodecyl sulfonate by adding Ca^{2+} [45]. The lifetimes of the salt bridges are longer for counterions that have higher binding fractions, Ca^{2+}, Li^+, and Ba^{2+}, than those of Na^+ and K^+, which is in agreement with molecular dynamics simulation results of studying the behavior of SDS micelles in the presence of excess NaCl or $CaCl_2$. Comparing with NaCl, $CaCl_2$ can result in more compact and rigidity of the SDS aggregates arises from relatively long-lived (~0.5 ns) salt bridges between nearest-neighbor headgroups, while the salt bridge mediated by Na^+ is typically tens of picoseconds in duration [46]. In addition to the binding free energy the off-rate of binding was used to evaluate the binding competition of cations to POPG lipid bilayer [47]. Similarly, the rigidity of salt bridges was quantificationally compared by break rates in the presenting study. The break rates of the most rigid salt bridges mediated by Ca^{2+} are 1–2 orders of magnitude smaller than those mediated by K^+.

5. Conclusion

The binding of ionized surfactin monolayer formed at the air/water interface to three monovalent counterions, Li^+, Na^+, and K^+ (molar ratio of surfactin to monovalent counterions is 1:2), and two divalent counterions, Ca^{2+} and Ba^{2+} (molar ratio of surfactin to divalent counterions is 1:1), has been investigated by all-atomistic molecular dynamics simulation. The results show that the positions of hydration layer of carboxyl groups are independent of counterions, but the bound counterions induce the dehydration of carboxyl groups and thus the fewer and less stable hydrogen bonds between carboxyl group and hydration water. Surfactin exhibits higher binding affinity to divalent counterions, Ca^{2+} and Ba^{2+}, and smaller monovalent counterion, Li^+, than Na^+ and K^+. The binding affinity can be attributed to the higher valence and bigger radius of divalent counterions which can be intensively bound and facilitate the formation of salt bridge between carboxyl groups, and the smaller cavity needed by Li^+ to interact with carboxyl groups as well as the weaker repulsion between the bound Li^+ ions. Both carboxyl groups are accessible for counterions, but carboxyl group in Glu1 is easier for counterions to access than Asp5. Salt bridges are widely detected in the presence of either monovalent counterions or divalent counterions, and the number of intermolecular salt bridge is markedly more than that of intramolecular salt bridge. Divalent counterions perform well in forming salt bridge between carboxyl groups within one surfactin or between surfactin ions. The most rigid salt bridges are mediated by Ca^{2+} and own lifetimes about 0.13 ns, and the break rates are in an order of 10^{-3} ps^{-1} which are 1–2 orders of magnitude smaller than those salt bridge mediated by K^+ which are about 5 ps in duration.

Acknowledgements

This work was financially supported by the National Science Foundation of China (21203063), the 863 Program (2013AA064403) and the Fundamental Research Funds for the Central Universities of China (nos. WK1213003, WJ1214066).

Appendix A. Supplementary data

Supplementary data to this article can be found online at http://dx.doi.org/10.1016/j.bbamem.2015.05.016.

References

[1] X.Y. Liu, S.Z. Yang, B.Z. Mu, Isolation and characterization of a C12-lipopeptide produced by *Bacillus subtilis* HSO121, J. Pept. Sci. 14 (2008) 864–875.
[2] N. Hue, L. Serani, O. Laprevote, Structural investigation of cyclic peptidolipids from *Bacillus subtilis* by high-energy tandem mass spectrometry, Rapid Commun. Mass Spectrom. 15 (2001) 203–209.
[3] J. Chakraborty, S. Chakrabarti, S. Das, Characterization and antimicrobial properties of lipopeptide biosurfactants produced by *Bacillus subtilis* sj301 and *Bacillus vallismortis* jb201, Appl. Biochem. Microbiol. 50 (2014) 609–618.
[4] R. Sahnoun, I. Minf, H. Fetoui, R. Gdoura, K. Chaabouni, F. Makni-Ayadi, C. Kallel, S. Ellouze-Chaabouni, D. Ghribi, Evaluation of *Bacillus subtilis* spb1 lipopeptide biosurfactant toxicity towards mice, Int. J. Pept. Res. Ther. 20 (2014) 333–340.
[5] A.K. Singh, S.S. Cameotra, Efficiency of lipopeptide biosurfactants in removal of petroleum hydrocarbons and heavy metals from contaminated soil, Environ. Sci. Pollut. Res. 20 (2013) 7367–7376.
[6] S.Y. Park, J.H. Kim, S.J. Lee, Y. Kim, Surfactin exhibits neuroprotective effects by inhibiting amyloid beta-mediated microglial activation, Neurotoxicology 38 (2013) 115–123.
[7] H. Amani, M. Haghighi, M.J. Keshtkar, Production and optimization of microbial surfactin by *Bacillus subtilis* for ex situ enhanced oil recovery, Pet. Sci. Technol. 31 (2013) 1249–1258.
[8] Y. Ishigami, M. Osman, H. Nakahara, Y. Sano, R. Ishiguro, M. Matsumoto, Significance of β-sheet formation for micellization and surface adsorption of surfactin, Colloids Surf. B 4 (1995) 341–348.
[9] F. Peypoux, J.M. Bonmatin, J. Wallach, Recent trends in the biochemistry of surfactin, Appl. Microbiol. Biotechnol. 51 (1999) 553–563.
[10] D. Vollenbroich, M. Ozel, J. Vater, R.M. Kamp, G. Pauli, Mechanism of inactivation of enveloped viruses by the biosurfactant surfactin from *Bacillus subtilis*, Biologicals 25 (1997) 289–297.
[11] S.R. Tendulkar, Y.K. Saikumari, V. Patel, S. Raghotama, T.K. Munshi, P. Balaram, B.B. Chattoo, Isolation, purification and characterization of an antifungal molecule produced by *Bacillus licheniformis* bc98, and its effect on phytopathogen *Magnaporthe grisea*, J. Appl. Microbiol. 103 (2007) 2331–2339.
[12] M. Kracht, H. Rokos, M. Ozel, M. Kowall, G. Pauli, J. Vater, Antiviral and hemolytic activities of surfactin isoforms and their methyl ester derivatives, J. Antibiot. 52 (1999) 613–619.
[13] J.M. Bonmatin, M. Genest, H. Labbe, M. Ptak, Solution three-dimensional structure of surfactin: a cyclic lipopeptide studied by ^{1}H-NMR, distance geometry, and molecular dynamics, Biopolymers 34 (1994) 975–986.
[14] R. Maget-Dana, M. Ptak, Interfacial properties of surfactin, J. Colloid Interface Sci. 153 (1992) 285–291.
[15] C.S. Song, R.Q. Ye, B.Z. Mu, Molecular behavior of a microbial lipopeptide monolayer at the air–water interface, Colloids Surf. A 302 (2007) 82–87.
[16] H.H. Shen, T.W. Lin, R.K. Thomas, D.J. Taylor, J. Penfold, Surfactin structures at interfaces and in solution: the effect of pH and cations, J. Phys. Chem. B 115 (2011) 4427–4435.
[17] Y. Li, A.H. Zou, R.Q. Ye, B.Z. Mu, Counterion induced changes to the micellization of surfactin–c16 aqueous solution, J. Phys. Chem. B 113 (2009) 15272–15277.
[18] A. Knoblich, M. Matsumoto, R. Ishiguro, K. Murata, Y. Fujiyoshi, Y. Ishigami, M. Osman, Electron cryo-microscopic studies on micellar shape and size of surfactin, an anionic lipopeptide, Colloids Surf. B 5 (1995) 43–48.
[19] J. Arutchelvi, J. Sangeetha, J. Philip, M. Doble, Self-assembly of surfactin in aqueous solution: role of divalent counterions, Colloids Surf. B 116 (2014) 396–402.
[20] L. Thimon, F. Peypoux, G. Michel, Interactions of surfactin, a biosurfactant from *Bacillus subtilis*, with inorganic cations, Biotechnol. Lett. 14 (1992) 713–718.
[21] M. Bortolato, F. Besson, B. Roux, Inhibition of alkaline phosphatase by surfactin, a natural chelating lipopeptide from *Bacillus subtilis*, Biotechnol. Lett. 19 (1997) 433–435.
[22] J. Penfold, R.K. Thomas, H.H. Shen, Adsorption and self-assembly of biosurfactants studied by neutron reflectivity and small angle neutron scattering: glycolipids, lipopeptides and proteins, Soft Matter 8 (2012) 578–591.
[23] W. Humphrey, A. Dalke, K. Schulten, VMD: visual molecular dynamics, J. Mol. Graph. 14 (1996) 33–38.
[24] A. Gilardoni, G. Gabrielli, Interfacial properties of surfactin, Progr. Colloid Polym. Sci. 93 (1993) 230–233.
[25] S.A. Onaizi, M.S. Nasser, F. Twaiq, Adsorption and thermodynamics of biosurfactant, surfactin, monolayers at the air–buffered liquid interface, Colloid Polym. Sci. 292 (2014) 1649–1656.

[26] J.P. Nicolas, Molecular dynamics simulation of surfactin molecules at the water–hexane interface, Biophys. J. 85 (2003) 1377–1391.
[27] H.Z. Gang, J.F. Liu, B.Z. Mu, Molecular dynamics study of surfactin monolayer at the air/water interface, J. Phys. Chem. B 115 (2011) 12770–12777.
[28] H.J.C. Berendsen, J.P.M. Postma, W.F. van Gunsteren, J. Hermans, Interaction Models for Water in Relation to Protein Hydration. Intermolecular forces, in: B. Pullman (Ed.), 14, D. Reidel Publishing Company, Dordrecht 1981, pp. 331–342.
[29] H.J.C. Berendsen, D. van der Spoel, R. van Drunen, Gromacs: a message-passing parallel molecular dynamics implementation, Comput. Phys. Commun. 91 (1995) 43–56.
[30] E. Lindahl, B. Hess, D. van der Spoel, Gromacs 3.0: a package for molecular simulation and trajectory analysis, J. Mol. Model. 7 (2001) 306–317.
[31] W.L. Jorgensen, D.S. Maxwell, J. Tiradorives, Development and testing of the OPLS all-atom force field on conformational energetics and properties of organic liquids, J. Am. Chem. Soc. 118 (1996) 11225–11236.
[32] H.J.C. Berendsen, J.P.M. Postma, W.F. van Gundteren, A. DiNola, J.R. Haak, Molecular dynamics with coupling to an external bath, J. Chem. Phys. 81 (1984) 3684–3690.
[33] U. Essmann, L. Perera, M.L. Berkowitz, T. Darden, H. Lee, L.G. Pedersen, A smooth particle mesh Ewald method, J. Chem. Phys. 103 (1995) 8577–8593.
[34] B. Hess, H. Bekker, H.J.C. Berendsen, J.G.E.M. Fraaije, Lincs: a linear constraint solver for molecular simulations, J. Comput. Chem. 18 (1997) 1463–1472.
[35] H.Z. Gang, J.F. Liu, B.Z. Mu, Interfacial behavior of surfactin at the decane/water interface: a molecular dynamics simulation, J. Phys. Chem. B 114 (2010) 14947–14954.
[36] D.C. Rapaport, Hydrogen bonds in water network organization and lifetimes, Mol. Phys. 50 (1983) 1151–1162.
[37] A. Chandra, Dynamical behavior of anion–water and water–water hydrogen bonds in aqueous electrolyte solutions: a molecular dynamics study, J. Phys. Chem. B 107 (2003) 3899–3906.
[38] S. Bandyopadhyay, S. Chakraborty, B. Bagchi, Secondary structure sensitivity of hydrogen bond lifetime dynamics in the protein hydration layer, J. Am. Chem. Soc. 127 (2005) 16660–16667.
[39] T.T. Zhao, G.Y. Xu, Y.J. Chen, H. Yan, Molecular dynamics study of alkyl benzene sulfonate at air/water interface: effect of inorganic salts, J. Phys. Chem. B 114 (2010) 5025–5033.
[40] V.E. Haverd, H.H. Warr, Cation selectivity at air/anionic surfactant solution interfaces, Langmuir 16 (2000) 157–160.
[41] M. Rautenbach, P. Swart, M.J. van der Merwe, The interaction of analogues of the antimicrobial lipopeptide, iturin a2, with alkali metal ions, Bioorg. Med. Chem. 8 (2000) 2539–2548.
[42] A. Grau, J.C. Gomez Fernandez, F. Peypoux, A. Ortiz, A study on the interactions of surfactin with phospholipid vesicles, Biochim. Biophys. Acta 1418 (1999) 307–319.
[43] S. Buchoux, J. Lai-Kee-Him, M. Garnier, P. Tsan, F. Besson, A. Brisson, E.J. Dufourc, Surfactin-triggered small vesicle formation of negatively charged membranes: a novel membrane-lysis mechanism, Biophys. J. 95 (2008) 3840–3849.
[44] H.H. Shen, R.K. Thomas, C.Y. Chen, R.C. Darton, S.C. Baker, J. Penfold, Aggregation of the naturally occurring lipopeptide, surfactin, at interfaces and in solution: an unusual type of surfactant, Langmuir 25 (2009) 4211–4218.
[45] H. Yan, X.L. Guo, S.L. Yuan, C.B. Liu, Molecular dynamics study of the effect of calcium ions on the monolayer of SDC and SDSN surfactants at the vapor/liquid interface, Langmuir 27 (2011) 5762–5771.
[46] M. Sammalkorpi, M. Karttunen, M. Haataja, Ionic surfactant aggregates in saline solutions: sodium dodecyl sulfate (SDS) in the presence of excess sodium chloride (NaCl) or calcium chloride ($CaCl_2$), J. Phys. Chem. B 113 (2009) 5863–5870.
[47] Y.Y. Mao, Y. Du, X.H. Cang, J.N. Wang, Z.X. Chen, H.Y. Yang, H.L. Jiang, Binding competition to the POPG lipid bilayer of Ca^{2+}, Mg^{2+}, Na^{+}, and K^{+} in different ion mixtures and biological implication, J. Phys. Chem. B 117 (2013) 850–858.